

Extracting α_S at future e^+e^- Higgs factory with energy correlators

Zhen Lin,^{1,*} Manqi Ruan,^{2,†} Meng Xiao,^{1,3,‡} and Zhen Xu^{1,§}

¹*Zhejiang Institute of Modern Physics, Department of Physics, Zhejiang University, Hangzhou, Zhejiang 310027, China*

²*Institute of High Energy Physics, Chinese Academy of Sciences, 19B Yuquan Road, Shijingshan District, Beijing 100049, China*

³*Center for high energy physics in Peking University, Beijing 100871, China*

(Dated: March 10, 2025)

The prospected sensitivity in α_S determination using an event shape observable, ratio of energy correlators at future electron-positron colliders is presented. The study focuses on the collinear region which has suffered from large theoretical and hadronization uncertainty in the past. The ratio effectively reduces the impacts of the uncertainties. With the amount of data that future electron-positron colliders could produce in 1 minute (40 pb^{-1}), a 1-2% precision of α_S could be reached depending on the hadronization uncertainty considered.

I. Introduction

The strong coupling constant (α_S) is a fundamental parameter in Quantum Chromodynamics (QCD). Its value enters theoretical predictions of strong interactions and its extraction requires experimental inputs. The current determination of α_S at the Z boson mass m_Z has a relative uncertainty of about 1% (0.1180 ± 0.0009) [1]. Compared to other constants that describe the strength of fundamental interaction, e.g. the fine-structure constant which characterizes the strength of the electroweak interaction [2], the precision of α_S is worse by several orders of magnitude. The limited precision of α_S has become one of the dominant uncertainties in the calculations of the Higgs process [3, 4]. It also affects the calculation of the partial widths of the Higgs boson decay [4–6] and plays a crucial role in determining quantities associated with the top quark, such as its mass, width, and Yukawa coupling [7, 8]. This imprecision motivates further improvements to enhance our understanding of QCD.

Various techniques have been deployed to determine α_S . At e^+e^- colliders, the analyses of event shapes in hadronic final states [9–18] have yielded important results. Event shapes are particularly sensitive to soft and collinear physics, which is crucial for refining the precision of α_S extraction and facilitating cross-checks with other methods. However, the particular phase space also introduces higher uncertainties: the calculation suffers from additional resummation uncertainties compared to fixed-order calculations. Moreover, the hadronization corrections in this region are often substantial, increasing the non-perturbative uncertainties as well. For these reasons, the previous extraction of α_S using energy energy correlators (E2C) at LEP explored data in the less

collinear region [18]. However the collinear region has rather substantial statistics, it would be beneficial to fully exploit it.

Recently the ratio between the projected three-point energy correlator (E3C) and E2C have proposed to extract α_S in the collinear region [19]. This has been performed by CMS experiment [20] and proved to effectively reduce hadronization uncertainty. In this study, we evaluate the feasibility of applying the method in the collinear region at e^+e^- collider at a center-of-mass energy of $\sqrt{s} = 91.2 \text{ GeV}$. The expected sensitivity of α_S is estimated including detector effects, theoretical and hadronization uncertainties. Experimental uncertainties are found to be minor. We present the expected precision of $\alpha_S(m_Z)$ at a luminosity of 40 pb^{-1} , which is similar to the combined luminosity used in previous E2C based determinations [18]. We exploit different ways to evaluate the hadronization uncertainty. A relative precision of 0.8% in $\alpha_S(m_Z)$ is obtained when adopting the traditional approach of evaluating Monte Carlo (MC) hadronization uncertainties through model comparisons. However, with more comprehensive decomposition of the uncertainties into multiple sources - including parameter tuning, parton shower (PS) scales and models, hadronization models, color reconnection and generator differences - the estimated precision is 1.5%. Taking into account the difference between analytical and MC based predictions, the expected precision becomes 2.1%.

II. Energy correlators and theoretical predictions

Energy correlators were designed to study the energy flow in an event or a jet [21]. The definition is adapted in different colliders [19]. At e^+e^- collider where the energy scale of hard scattering is fixed, the energy correlators describe the energy-weighted angular distances among all the final particles in an event. The simplest energy correlator is E2C, defined as

* zhenlin@zju.edu.cn
† ruanmq@ihep.ac.cn
‡ mxiao@zju.edu.cn
§ zhen.xu@zju.edu.cn

$$\text{E2C} = \frac{d\sigma^{[2]}}{dx_L} = \sum_{i,j}^n \int d\sigma \frac{E_i E_j}{Q^2} \delta(x_L - \frac{1 - \cos \chi_{ij}}{2}), \quad (1)$$

where the χ is the angular distance between particle i, j , and the energy of the two particles are denoted by E_i, E_j . The E2C observable was extensively studied at early e^+e^- colliders [22–32]. A previous study has used E2C measurement to extract α_S by comparing it to theoretical calculations at NNLO + NNLL precision [18]. Due to the large uncertainty in both theoretical prediction and hadronization corrections in the collinear region, only the intermediate region data was used, corresponding to χ between 60° to 160° . The determined result was $\alpha_S(m_Z) = 0.1175 \pm 0.00018(\text{exp.}) \pm 0.00102(\text{hadr.}) \pm 0.00257(\text{ren.}) \pm 0.00078(\text{res.})$. Even so, the theoretical and hadronization uncertainties are notably larger compared to the experimental ones.

To mitigate such limitation, the ratio of E3C to E2C has been proposed to extract α_S in the collinear region [19]. The E3C is an energy correlator that captures the correlation among three particles, defined as

$$\text{E3C} = \frac{d\sigma^{[3]}}{dx_L} = \sum_{i,j,k}^n \int d\sigma \frac{E_i E_j E_k}{Q^3} \delta\left(x_L - \max\left(\frac{1 - \cos \chi_{ij}}{2}, \frac{1 - \cos \chi_{ik}}{2}, \frac{1 - \cos \chi_{jk}}{2}\right)\right). \quad (2)$$

The ratio of E3C/E2C has minimal non-singular contributions in the collinear limit and allows for safe neglect of higher fixed-order corrections. It also diminishes non-perturbative effects and the associated uncertainties. In order to estimate the sensitivity to α_S using the E3C/E2C, we calculate the E3C and E2C at NLO+NNLL precision using the methodology introduced in Ref. [33], at a center-of-mass energy of $\sqrt{s} = 91.2$ GeV in e^+e^- colliders. It would be interesting to consider the matching to NNLO correction which is available for E2C since Ref.[34] and can be calculated in principle with the methods in Ref.[35] and Ref.[34]. However, such a calculation is computationally expensive. We also found that while the matching effect from LO to NLO is non-negligible on E2C and E3C respectively, the effect on the ratio is small, especially in the collinear region. Therefore we expect the correction due to further NNLO matching to be minor.

We consider the χ angles in the collinear region, from 6° to 60° , corresponding to $x_L = (1 - \cos \chi)/2$ in the range of 0.003–0.25. The predicted E3C/E2C distribution at the parton level with different $\alpha_S(m_Z)$ values are shown in Fig. 1. A variation of 3% in α_S leads to an approximate 2% change in the E3C/E2C ratio.

In the next sections, we will discuss in detail the different types of uncertainties that enter α_S determination using E3C/E2C ratio.

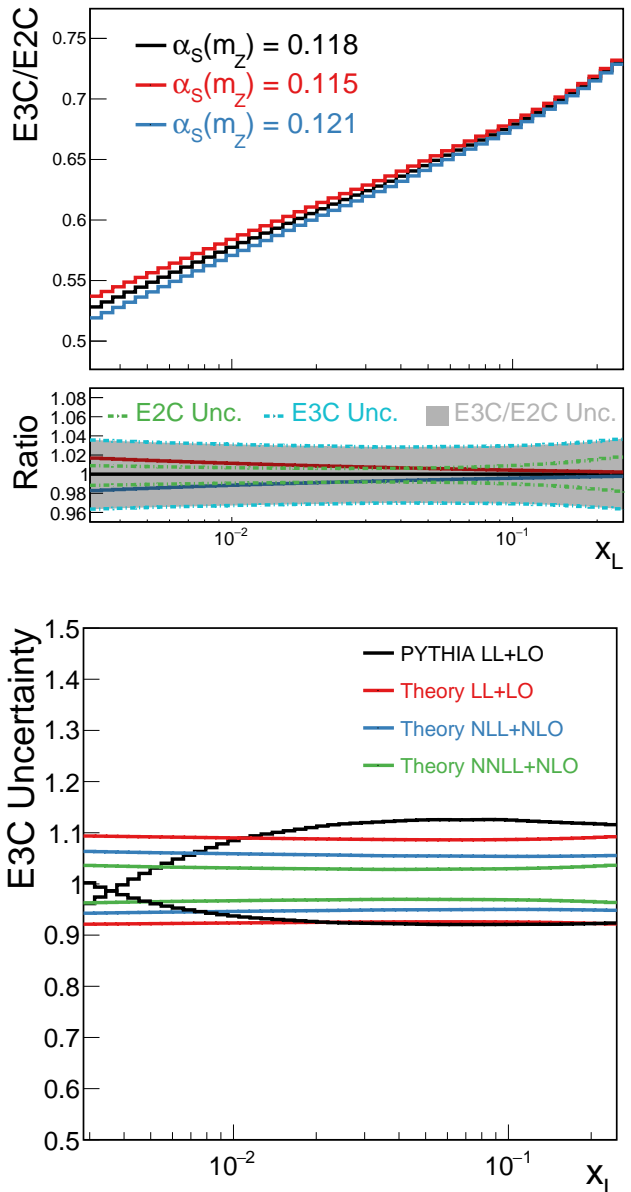


FIG. 1: Top: Theoretical prediction of E3C/E2C for different $\alpha_S(m_Z)$ values. The lower panel shows the ratio to $\alpha_S(m_Z) = 0.118$ prediction. Uncertainties of E2C, E3C and their ratio are shown at $\alpha_S(m_Z) = 0.118$.

Bottom: E3C uncertainty derived from PYTHIA simulation and theoretical calculations at different orders.

III. Theoretical scale uncertainties

For theoretical predictions of E2C and E3C at NLO + NNLL precision, there are two scales that enter the calculation: the hard scale and jet scale. In some earlier studies [18], the two scales were varied independently to evaluate the theoretical uncertainties from missing higher

order corrections. However, for the calculation used here, resummation is performed by iteratively solving the jet function RG equation to order $O(\alpha_S^{50})$. Therefore the prediction is regarded as truncated perturbative expansion, where the jet scale and hard scale are related by $\mu_j = \mu_h \sqrt{x_L}$, leaving a single hard scale $\mu_h = \mu$ in the expression. The theoretical uncertainty is therefore evaluated by varying the hard scale μ by 1/2 and 2. More detailed discussion on the scale uncertainty could be found in Ref. [33].

The individual theoretical scale uncertainties of E2C and E3C are shown in Fig. 1 ratio panel. As a comparison, we show the scale uncertainty in PYTHIA 8.306 [36] simulation in the bottom plot of Fig. 1, which is at LO+LL, obtained from varying the PS scales of both final state radiation (FSR) and initial state radiation (ISR) by 1/2 and 2. The PYTHIA PS scale uncertainty is compatible with the theoretical uncertainty at LO+LL precision by varying the hard scale described above. The theoretical scale uncertainties at different perturbative and resummation orders are also shown, where a decrease from 10% at LO+LL order to 4% at NLO+NNLL order is seen. The uncertainty in the E3C/E2C ratio, is obtained from a seven-point scale variation method, where the scales of the E2C and E3C are varied independently by a factor of 1/2 and 2, while keeping their ratio between 1/2 and 2. The uncertainty of the ratio is shown as grey band in Fig. 1 top plot. As seen in the ratio panel, taking the ratio does not cancel out scale uncertainties.

IV. Non-perturbative effects and uncertainties

An important aspect of event-shape based α_S extraction is the evaluation of non-perturbative corrections. Approaches to derive these corrections can be classified into two general categories: MC based [18, 37–42] and analytical model based [43–50], which do not always yield the same result. In this study, we explore several options in both methods to evaluate the hadronization effects and compare their ultimate impacts on the α_S extraction.

For the analytical model based approach, we used the non-perturbative power correction provided by Ref. [44]. It is denoted as Ω in this paper. For the MC based approaches, the effect is extracted from the distributions predicted by MC at hadron level divided by those at parton level. As there are a variety of models in MC generators, a two-point model uncertainty is usually adopted, where all the aspects of generator setups are varied simultaneously, and the difference, for example, by changing from PYTHIA to HERWIG is taken as the uncertainty. Recent guidelines established by Les Houches community [51] have pointed out that a more factorized two-point comparison is needed to assess the different aspects of non-perturbative effects, as has been done by ATLAS collaboration in the jet energy scale uncertainty determination [52, 53]. Therefore, we try to decompose possible factors in non-perturbative corrections, and evaluate the

respective uncertainties either by varying parameters or by utilizing two-point comparisons of settings for a single aspect. The list of factors considered includes:

- **PS scale:** PS scale changes the prediction at both parton level and hadron level, and the yielded hadronization correction could be different. We vary the renormalization scales of FSR and ISR independently by factors of 1/2 and 2 from their nominal values, each time a new hadronization correction is calculated, and the uncertainty is obtained from a seven-point scale envelope. This uncertainty is evaluated in PYTHIA simulation.
- **PS model:** Multiple PS models are available in MC generators. The mostly commonly adopted ones include the p_T -ordered PS implemented in PYTHIA, the angular-ordered PS [54] based on coherent branching implemented in HERWIG 7.2.2 [55], and the Catani-Seymour (CS) dipole PS [56–58] implemented in both HERWIG and SHERPA 2.2.12 [59, 60] with customized settings. To isolate the effect of different PS model, we keep the rest of configurations, such as hadronization model and tune parameters the same. This is realized by using HERWIG simulation, where angular ordered and CS dipole PS are compared while keeping the other settings fixed.
- **Hadronization model:** Two general types of hadronization models are widely used in MC generators: the Lund string model [61, 62], which is deployed in PYTHIA and SHERPA, and the cluster-based model [63] deployed in HERWIG and SHERPA. To evaluate the sole effect of hadronization model, two SHERPA simulations are compared where the CS dipole PS is interfaced with either the cluster-based AHADIC++ model or the Lund string model.
- **Generator:** Even if the general parton shower and hadronization models are the same in different MC generators, the derived hadronization correction could differ due to internal optimizations. This additional uncertainty is determined by comparing HERWIG with SHERPA, where both simulations use CS dipole shower and cluster hadronization models.
- **Tune:** For hadronization, each generator has its own default set of tune parameters. PYTHIA provided multiple parameter sets that were derived by different methods. We tested all the seven choices called by Tune:ee method in PYTHIA, which were tuned to e^+e^- data. The two choices that result in the largest difference in hadronization correction: the default Monash tune optimized for both e^+e^- and pp collisions, and the Tune:ee = 6 are taken as the tune uncertainty.

| Generator | PS model | Hadronization model | Tune | PS scale | CR |
|---------------|-----------------|---------------------|---------------|-----------|------------------------------|
| PYTHIA 8.306 | p_T -ordered | Lund string | Monash tune | 1/2, 1, 2 | MPI, GM, CS |
| PYTHIA 8.306 | p_T -ordered | Lund string | Tune:ee = 1-6 | 1 | MPI |
| HERWIG 7.2.2 | Angular-ordered | Cluster | Default | 1 | Baryonic, plain, statistical |
| HERWIG 7.2.2 | CS dipole | Cluster | Default | 1 | Baryonic |
| SHERPA 2.2.12 | CS dipole | Cluster (AHADIC++) | Retuned | 1 | Default |
| SHERPA 2.2.12 | CS dipole | Lund string | Default | 1 | Default |

TABLE I: Overview of the generated MC samples. Detailed configurations of the PS, hadronization, tune and CR models are listed.

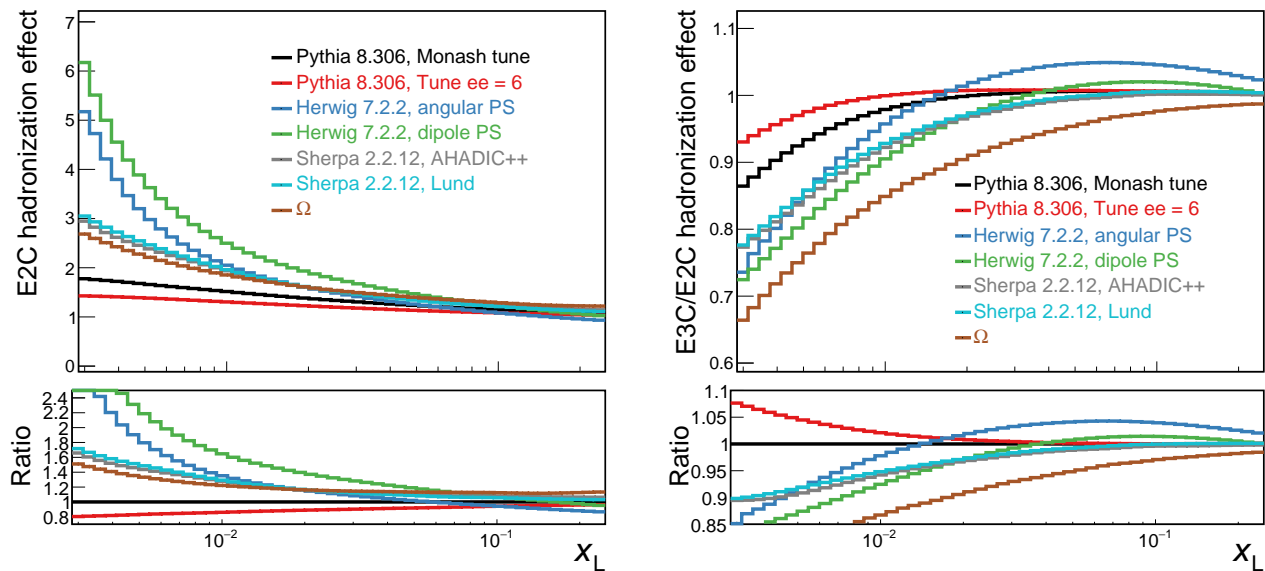


FIG. 2: Hadronization correction factors for E2C (left) and E3C/E2C (right), derived from various MC generators and settings.

- Color reconnection (CR):** Although it is believed that CR has a small impact in e^+e^- colliders, we explicitly tested it by employing different CR models. This is assessed by comparing the default baryonic model with plain and statistical models in HERWIG. A similar comparison is performed between the default MPI-based model with GM and CS models in PYTHIA. Both are found to have small effect on the hadronization correction (less than 0.5%). The slightly more pronounced difference between the baryonic model and the two other models in HERWIG is taken as the CR uncertainty.

Events of $e^+e^- \rightarrow qq$ at $\sqrt{s} = 91.2$ GeV are simulated. This energy has the benefit of a high cross-section of the two-quark final state and negligible background contribution. We employ three event generators: PYTHIA 8.306, HERWIG 7.2.2, and SHERPA 2.2.12, each implementing distinct approaches to parton showering and hadronization

to assess the various factors introduced above.

We use PYTHIA 8.306 with a p_T -ordered parton shower, combined with Lund string hadronization model to evaluate the PS scale and tune uncertainties. Monash 2013 tune [64] is used as the nominal setting. HERWIG 7.2.2 offers two complementary parton shower algorithms: the angular-ordered shower and CS dipole shower. Both algorithms are interface with HERWIG's cluster hadronization model to evaluate the PS model uncertainty. The default tune is used. SHERPA 2.2.12 with CS dipole PS interfaced with two different hadronization models, its native AHADIC++ cluster approach [65], and the Lund string model, to extract the hadronization model uncertainty. The former configuration incorporates specially optimized tune parameters [53, 66] validated against LEP data on jet hadron composition. This tune is found to have negligible impact on the hadronization correction. A summary of all the simulated samples with the key configurations are listed in Tab. I.

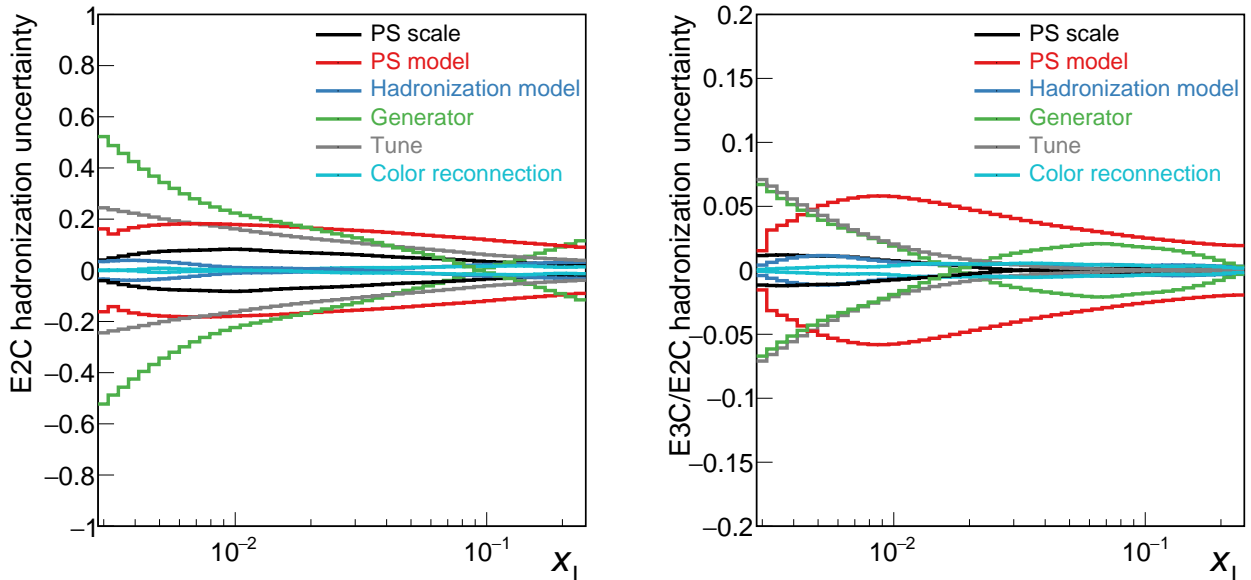


FIG. 3: Hadronization uncertainty breakdown for E2C (left) and E3C/E2C (right).

The hadronization correction derived from various MC generators, as well as Ω from the analytical method, for E2C and E3C/E2C are shown in Fig. 2. The correction is much more pronounced in E2C, particularly in the small x_L region. The differences between MC generators also increase towards collinear region. Using the E3C/E2C ratio largely reduces the scale of the correction, as well as the dependency on different models, which amounts to 200% in E2C and reduces to 20% in the E3C/E2C ratio. It is also noted that the analytical correction Ω is not close to any of the MC based corrections in E3C/E2C variable.

The breakdown of the individual factors that affects the MC hadronization correction is extracted as described above, either from parameter variation, or from two-point comparisons between different settings. Figure 3 presents the individual source of hadronization uncertainties on E2C (left) and E3C/E2C ratio (right). As expected, each single uncertainty decreases as x_L increases and gets significantly smaller switching from E2C to E3C/E2C. Among all the factors, the tune parameter and the generator differences play major roles in the most collinear region, and the PS model becomes dominant in the slightly larger x_L region. PS scale, hadronization model and CR model uncertainties are smaller in size, all within 2% for E3C/E2C. However, we would like to point out that when it comes to α_S extraction, not only the size of the uncertainty, but also the shape is important, as all the bins are treated correlated.

V. Detector effects and experimental uncertainties

Before estimating the α_S sensitivity, we assess the detector effects in realistic experimental conditions. Monte Carlo events are generated using PYTHIA8.306 with p_T -ordered PS, Lund string hadronization model and Monash tune, followed by detector simulation through Delphes [67], implementing both CEPC [68] and FCC-ee [69] detector configurations. The CEPC detector design has an Electromagnetic Calorimeter (ECAL) with an energy resolution of approximately $16\%/\sqrt{E}$, and a Hadronic Calorimeter (HCAL) achieving an energy resolution of around $50\%/\sqrt{E}$ [70]. The FCC-ee detector has a similar performance in its calorimetric system, with the ECAL achieving an energy resolution of $16.5\%/\sqrt{E}$, and the HCAL delivering a slightly improved resolution of $44.2\%/\sqrt{E}$ [71]. Both experiments employ the Particle Flow Algorithm (PFA) to optimize their detection capabilities and expect exceptional angular resolution for charged particles, reaching precisions of ≤ 0.1 mrad for momenta above 10 GeV [69, 72], which provides excellent precision for energy correlator measurements.

The detector effects are evaluated through the ratio of distributions at hadron level before and after the Delphes detector simulation. Figure 4 illustrates the detector effects on E2C and E3C/E2C ratio for CEPC and FCC-ee. The two experiments exhibit similar performances, the effect is between 5–10% for E2C depending on the x_L value. The experimental effect cancels out in the E3C/E2C ratio, both in magnitude and shape dependencies. The size is 1–3% for both experiments, with a slightly smaller size in CEPC. As the detector performances are rather similar, we use CEPC to evaluate

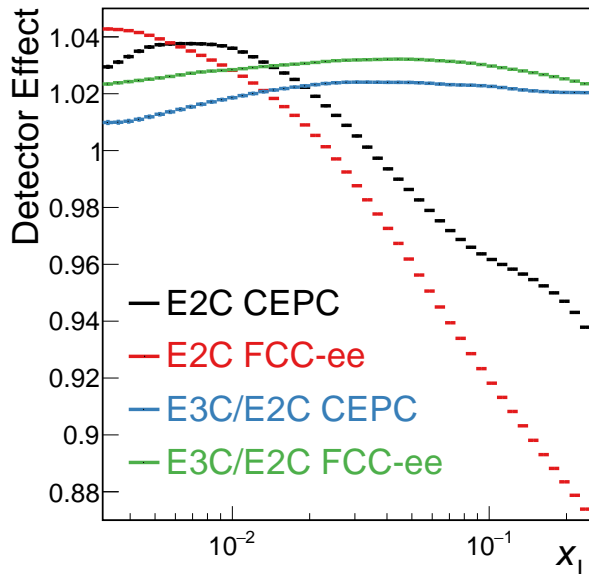


FIG. 4: Detector effects on the E2C and E3C/E2C in CEPC and FCCee.

potential experimental uncertainties and further demonstrate the expected sensitivity of α_S .

In earlier studies, CMS has extracted α_S from E3C/E2C and found the dominant experimental uncertainty being the energy scale of the composite particles [20]. Therefore we focus on these sources to evaluate the overall experimental uncertainty. Depending on the particles' types, the energy scale uncertainties at CMS are 1%, 3% and 5% for charged particles, photons and neutral particles, respectively. With the excellent tracker and calorimeter design of CEPC and FCCee, it is safe to assume the uncertainties could be reduced by half. We vary the energy scales of the individual particles entering the energy correlator calculation, and the impact of the uncertainties is presented in Fig. 5. For the E2C observable, the uncertainties are at the scale of 0.04%, with neutral hadrons being the largest source of uncertainty. The effect is further reduced in E3C/E2C ratio, only up to 0.01% level. This demonstrates the robustness of the observable against detector-related systematic uncertainties. Given that these uncertainties are several orders of magnitude smaller than the hadronization and theoretical uncertainties, we neglect their contribution in the subsequent α_S extraction.

VI. Expected sensitivity of α_S

We apply the hadronization and detector corrections to the above NLO + NNLL parton-level predictions at $\alpha_S(m_Z) = 0.118$ to obtain the pseudo data distributions of E3C/E2C. The hadronization factor is taken from PYTHIA and the detector effects are taken from CEPC

setting. The distributions are scaled to the luminosity of 40 pb^{-1} and compared to predictions under a set of different values of $\alpha_S(m_Z)$, where hadronization and detector effects are also propagated. The χ^2 between the pseudo data and the predictions are calculated to assess the expected sensitivity of α_S , including uncertainties in theoretical predictions discussed in Sec. III and hadronization effects. We compare three approaches in handling the hadronization uncertainty: scheme1 (S1) follows the traditional MC method, which takes the overall difference between predictions from HERWIG and PYTHIA generators, where all the default settings in the generators are taken; Scheme2 (S2) does a more detailed assessment by decomposing the MC based hadronization effects into six distinct sources of uncertainties as discussed in Sec. IV; Scheme3 (S3) tries to take into account the difference between the MC and analytical predictions. As there are no factorized way to evaluate the uncertainty, we take the difference between PYTHIA and Ω , and the difference between HERWIG and Ω as two independent systematic sources. The experimental uncertainties have shown a negligible impact and are safely discarded.

The bins in energy correlator distributions are not statistically independent. The correlation matrix among them is recorded and used in the χ^2 calculation, which is defined as

$$\chi^2(\alpha_S, \vec{\theta}) = \left(\vec{v}_{\text{th}}(\vec{\theta}, \alpha_S) - \vec{v}_{\text{data}}(\vec{\theta}) \right)^T V_{\text{data}}^{-1} \left(\vec{v}_{\text{th}}(\vec{\theta}, \alpha_S) - \vec{v}_{\text{data}}(\vec{\theta}) \right) + \sum_i \theta_i^2. \quad (3)$$

Here, \vec{v}_{th} represents the theoretical prediction of E3C/E2C distribution for various $\alpha_S(m_Z)$, and V_{data} is the covariance matrix derived from pseudo data. The hadronization and theoretical uncertainties enter the χ^2 as shape nuisance parameters $\vec{\theta} = (\theta_1, \theta_2)$, which means all the bins are varied correlatively under the uncertainties. Each changes the shape of E3C/E2C and constraint by a Gaussian distribution. The overall χ^2 is minimized floating $\vec{\theta}$ at each value of $\alpha_S(m_Z)$.

We extract the expected sensitivity of $\alpha_S(m_Z)$ from the χ^2 scan at an integrated luminosity of 40 pb^{-1} , which is comparable to the integrated luminosity used in the previous α_S extraction with the E2C observable [18] from e^+e^- data. The CEPC aims to collect a large dataset of 100 ab^{-1} over two years at $\sqrt{s} = 91.2 \text{ GeV}$ [73, 74], and the FCC-ee plans to take 150 ab^{-1} data in four years [69]. Therefore the considered luminosity could be achievable at both experiments in less than 1 minute.

Figure 6 shows the expected uncertainties on $\alpha_S(m_Z)$. The theoretical uncertainty contributes about 0.5% and the statistical uncertainty is 0.1%. The contribution of hadronization uncertainty as well as the overall expected sensitivity is shown separately in the three schemes. In S1, the same two-point hadronization uncertainty adopted by the previous e^+e^- E2C result is used. The

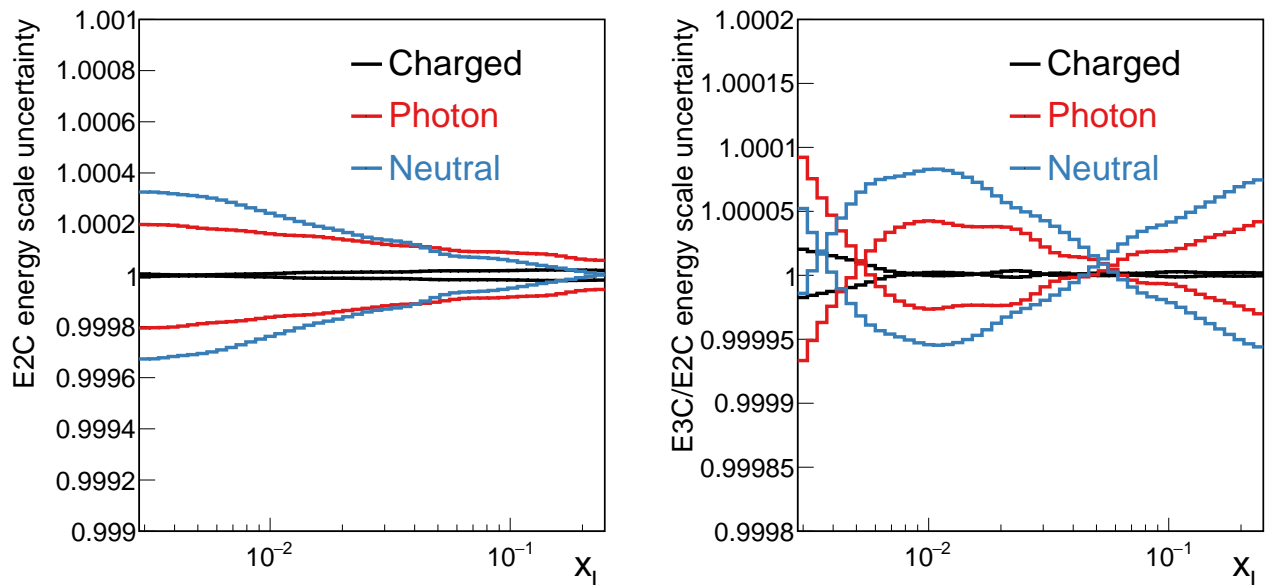


FIG. 5: Particle energy scale uncertainty for E2C (left) and E3C/E2C (right).

hadronization uncertainty using E3C/E2C is approximately 0.6%, yielding an overall sensitivity of 0.8%. This is significantly better than the 2.4% reported in the previous E2C result, illustrating the improved control over uncertainties offered by the E3C/E2C ratio observable. In S2, a more comprehensive decomposition of the hadronization effects is performed, and a larger hadronization uncertainty of 1.5% is obtained. The contribution of each single source is also shown in Fig. 6. All of them show sizable impacts on the α_S determination, among which the PS scale and tune settings contribute the most. The difference seen in S1 and S2 suggests that a simple two-point variation may underestimate the MC hadronization uncertainty. In S3, we see a large difference between analytical prediction Ω and PYTHIA, and the hadronization uncertainty reaches 2.1%.

With 40 pb^{-1} data, we see that the uncertainties of the theoretical prediction and the hadronization corrections are already dominated over statistical uncertainty. In particular, different treatment of the hadronization uncertainty could change the result significantly. Therefore extra efforts would be needed to understand these important effects and reduce the size of the relevant uncertainty in the future, to better exploit the large dataset going to be collected in e^+e^- colliders.

VII. Conclusion

In this study, we evaluate the sensitivity of α_S extraction at future e^+e^- colliders by using E3C/E2C ratio

observable in the collinear region, which has not been explored by previous event-shape based methods. This observable demonstrates substantial advantages, including minimal dependence on detector response and reduced hadronization effects. With NLO + NNLL precision calculation, several schemes for evaluating hadronization uncertainties are considered. In the traditional approach that only considers differences between Monte Carlo models like PYTHIA and HERWIG, the expected relative sensitivity could reach approximately 0.8% under a luminosity of 40 pb^{-1} . However, detailed decomposition into sources including parton shower scale and model, hadronization model, tune, color reconnection model and generator implementations, a more conservative sensitivity of 1.5% is expected. If the difference between analytical and MC based methods are considered, the sensitivity degrades to 2.1%. The study highlights the importance of understanding hadronization effects beyond simple model comparisons. The theoretical uncertainty, along with the hadronization uncertainty, have been shown to be the limiting factors in extracting α_S through energy correlators in future high luminosity e^+e^- colliders and a better understanding of them is in need.

Acknowledgements

We thank Huaxing Zhu for the useful discussions. The work is supported by National Natural Science Foundation of China (NSFC) under the Grant No. 12322504 and the Innovative Scientific Program of the Institute of High Energy Physics.

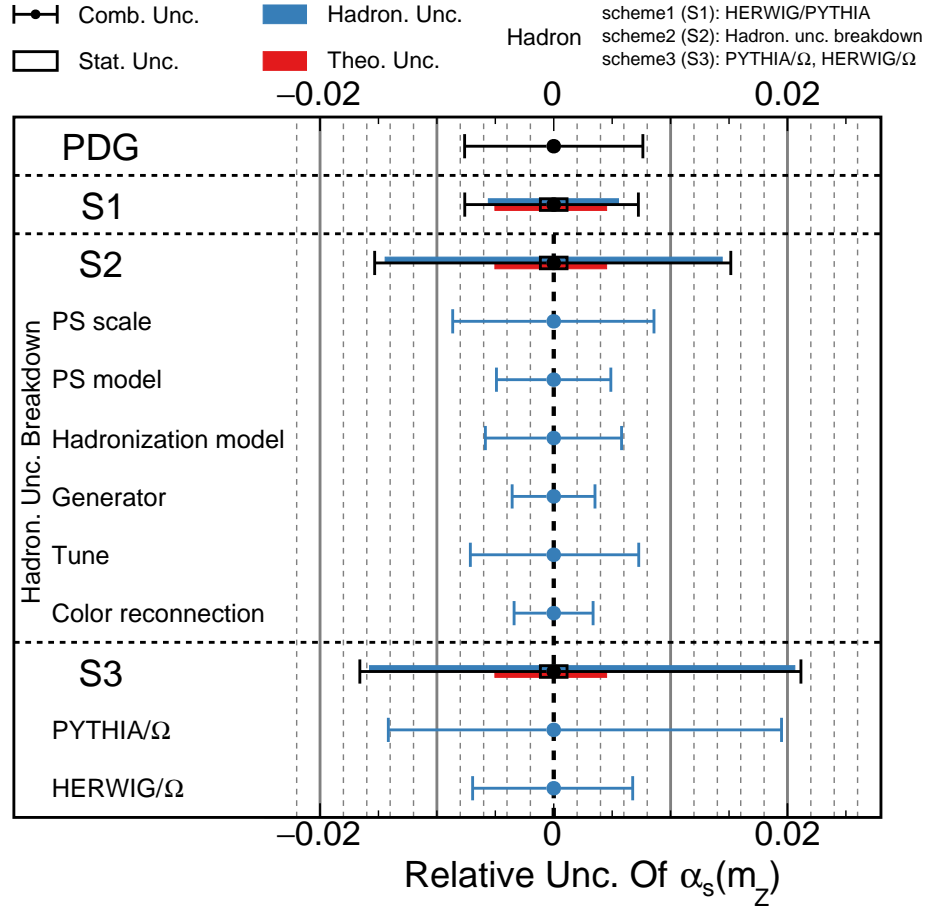


FIG. 6: The expected sensitivity to $\alpha_s(m_Z)$ using E3C/E2C at CEPC at 40 pb^{-1} . The PDG 2022 world average precision for α_s extraction is shown for a comparison [1]. The breakdown of statistical, hadronization, and theoretical uncertainties, as well as the combined results, are shown. Three approaches for evaluating hadronization uncertainties are presented. S1 uses the traditional method based on the difference between HERWIG and PYTHIA predictions. S2 employs a detailed decomposition into six distinct sources and the breakdown of these components is presented. S3 takes the difference between the analytical and MC based predictions.

- [1] R. L. Workman *et al.* (Particle Data Group), Review of Particle Physics, PTEP **2022**, 083C01 (2022).
- [2] E. Tiesinga, P. J. Mohr, D. B. Newell, and B. N. Taylor, CODATA recommended values of the fundamental physical constants: 2018*, Rev. Mod. Phys. **93**, 025010 (2021).
- [3] C. Anastasiou, C. Duhr, F. Dulat, E. Furlan, T. Gehrmann, F. Herzog, A. Lazopoulos, and B. Mistlberger, High precision determination of the gluon fusion Higgs boson cross-section at the LHC, JHEP **05**, 058, arXiv:1602.00695 [hep-ph].
- [4] D. de Florian *et al.* (LHC Higgs Cross Section Working Group), Handbook of LHC Higgs Cross Sections: 4. Deciphering the Nature of the Higgs Sector **2/2017**, 10.23731/CYRM-2017-002 (2016), arXiv:1610.07922 [hep-ph].
- [5] G. P. Lepage, P. B. Mackenzie, and M. E. Peskin, Expected Precision of Higgs Boson Partial Widths within the Standard Model, (2014), arXiv:1404.0319 [hep-ph].
- [6] A. Denner, S. Heinemeyer, I. Puljak, D. Reubuzzi, and M. Spira, Standard Model Higgs-Boson Branching Ratios with Uncertainties, Eur. Phys. J. C **71**, 1753 (2011), arXiv:1107.5909 [hep-ph].
- [7] A. H. Hoang, What is the Top Quark Mass?, Ann. Rev. Nucl. Part. Sci. **70**, 225 (2020), arXiv:2004.12915 [hep-ph].
- [8] A. M. Cooper-Sarkar, M. Czakon, M. A. Lim, A. Mitov, and A. S. Papanastasiou, Simultaneous extraction of α_s and m_t from LHC $t\bar{t}$ differential distributions, (2020), arXiv:2010.04171 [hep-ph].
- [9] G. Dissertori, A. Gehrmann-De Ridder, T. Gehrmann, E. W. N. Glover, G. Heinrich, G. Luisoni, and H. Stenzel, Determination of the strong coupling constant using matched NNLO+NLLA predictions for hadronic event shapes in e^+e^- annihilations, JHEP **08**, 036, arXiv:0906.3436 [hep-ph].
- [10] G. Abbiendi *et al.* (OPAL), Determination of α_s using OPAL hadronic event shapes at $\sqrt{s} = 91 - 209$ GeV and resummed NNLO calculations, Eur. Phys. J. C **71**, 1733 (2011), arXiv:1101.1470 [hep-ex].
- [11] S. Bethke, S. Kluth, C. Pahl, and J. Schieck (JADE), Determination of the Strong Coupling α_s from hadronic Event Shapes with $\mathcal{O}(\alpha_s^3)$ and resummed QCD predictions using JADE Data, Eur. Phys. J. C **64**, 351 (2009), arXiv:0810.1389 [hep-ex].
- [12] R. A. Davison and B. R. Webber, Non-Perturbative Contribution to the Thrust Distribution in e^+e^- Annihilation, Eur. Phys. J. C **59**, 13 (2009), arXiv:0809.3326 [hep-ph].
- [13] R. Abbate, M. Fickinger, A. H. Hoang, V. Mateu, and I. W. Stewart, Thrust at N^3LL with Power Corrections and a Precision Global Fit for $\alpha_s(m_Z)$, Phys. Rev. D **83**, 074021 (2011), arXiv:1006.3080 [hep-ph].
- [14] T. Gehrmann, G. Luisoni, and P. F. Monni, Power corrections in the dispersive model for a determination of the strong coupling constant from the thrust distribution, Eur. Phys. J. C **73**, 2265 (2013), arXiv:1210.6945 [hep-ph].
- [15] A. Kardos, G. Somogyi, and A. Verbytskyi, Determination of α_s beyond NNLO using event shape averages, Eur. Phys. J. C **81**, 292 (2021), arXiv:2009.00281 [hep-ph].
- [16] A. H. Hoang, D. W. Kolodrubetz, V. Mateu, and I. W. Stewart, Precise determination of α_s from the C -parameter distribution, Phys. Rev. D **91**, 094018 (2015), arXiv:1501.04111 [hep-ph].
- [17] G. Luisoni, P. F. Monni, and G. P. Salam, C -parameter hadronisation in the symmetric 3-jet limit and impact on α_s fits, Eur. Phys. J. C **81**, 158 (2021), arXiv:2012.00622 [hep-ph].
- [18] A. Kardos, S. Kluth, G. Somogyi, Z. Tulipánt, and A. Verbytskyi, Precise determination of $\alpha_s(M_Z)$ from a global fit of energy-energy correlation to NNLO+NNLL predictions, Eur. Phys. J. C **78**, 498 (2018), arXiv:1804.09146 [hep-ph].
- [19] H. Chen, I. Moulst, X. Y. Zhang, and H. X. Zhu, Rethinking jets with energy correlators: tracks, resummation, and analytic continuation, Phys. Rev. D **102**, 054012 (2020), arXiv:2004.11381 [hep-ph].
- [20] A. Hayrapetyan *et al.* (CMS), Measurement of Energy Correlators inside Jets and Determination of the Strong Coupling $\alpha_s(m_Z)$, Phys. Rev. Lett. **133**, 071903 (2024), arXiv:2402.13864 [hep-ex].
- [21] C. L. Basham, L. S. Brown, S. D. Ellis, and S. T. Love, Energy correlations in electron - positron annihilation: Testing QCD, Phys. Rev. Lett. **41**, 1585 (1978).
- [22] K. Abe *et al.* (SLD), Measurement of $\alpha_s(M(Z)^2)$ from hadronic event observables at the Z0 resonance, Phys. Rev. D **51**, 962 (1995), arXiv:hep-ex/9501003.
- [23] O. Adrian *et al.* (L3), Determination of α_s from hadronic event shapes measured on the Z0 resonance, Phys. Lett. B **284**, 471 (1992).
- [24] P. D. Acton *et al.* (OPAL), A Determination of $\alpha_s(M(Z))$ at LEP using resummed QCD calculations, Z. Phys. C **59**, 1 (1993).
- [25] I. Adachi *et al.* (TOPAZ), Measurements of α_s in e^+e^- Annihilation at $\sqrt{s} = 53.3$ -GeV and 59.5-GeV, Phys. Lett. B **227**, 495 (1989).
- [26] W. Braunschweig *et al.* (TASSO), A Study of Energy-energy Correlations Between 12-GeV and 46.8-GeV CM Energies, Z. Phys. C **36**, 349 (1987).
- [27] W. Bartel *et al.* (JADE), Measurements of Energy Correlations in $e^+e^- \rightarrow$ Hadrons, Z. Phys. C **25**, 231 (1984).
- [28] E. Fernandez *et al.*, A Measurement of Energy-energy Correlations in $e^+e^- \rightarrow$ Hadrons at $\sqrt{s} = 29$ -GeV, Phys. Rev. D **31**, 2724 (1985).
- [29] D. R. Wood *et al.*, Determination of α_s From Energy-energy Correlations in e^+e^- Annihilation at 29-GeV, Phys. Rev. D **37**, 3091 (1988).
- [30] H. J. Behrend *et al.* (CELLO), Analysis of the Energy Weighted Angular Correlations in Hadronic e^+e^- Annihilations at 22-GeV and 34-GeV, Z. Phys. C **14**, 95 (1982).
- [31] C. Berger *et al.* (PLUTO), A Study of Energy-energy Correlations in e^+e^- Annihilations at $\sqrt{s} = 34.6$ -GeV, Z. Phys. C **28**, 365 (1985).
- [32] P. Abreu *et al.* (DELPHI), Consistent measurements of α_s from precise oriented event shape distributions, Eur. Phys. J. C **14**, 557 (2000), arXiv:hep-ex/0002026.
- [33] W. Chen, J. Gao, Y. Li, Z. Xu, X. Zhang, and H. X. Zhu, NNLL resummation for projected three-point energy correlator, JHEP **05**, 043, arXiv:2307.07510 [hep-ph].

- [34] V. Del Duca, C. Duhr, A. Kardos, G. Somogyi, and Z. Trócsányi, Three-Jet Production in Electron-Positron Collisions at Next-to-Next-to-Leading Order Accuracy, *Phys. Rev. Lett.* **117**, 152004 (2016), arXiv:1603.08927 [hep-ph].
- [35] A. Gehrmann-De Ridder, T. Gehrmann, E. W. N. Glover, and G. Heinrich, NNLO corrections to event shapes in e^+e^- annihilation, *JHEP* **12**, 094, arXiv:0711.4711 [hep-ph].
- [36] C. Bierlich *et al.*, A comprehensive guide to the physics and usage of PYTHIA 8.3, *SciPost Phys. Codeb.* **2022**, 8 (2022), arXiv:2203.11601 [hep-ph].
- [37] A. Verbytskyi, A. Banfi, A. Kardos, P. F. Monni, S. Kluth, G. Somogyi, Z. Szőr, Z. Trócsányi, Z. Tulipánt, and G. Zanderighi, High precision determination of α_s from a global fit of jet rates, *JHEP* **08**, 129, arXiv:1902.08158 [hep-ph].
- [38] G. Dissertori, A. Gehrmann-De Ridder, T. Gehrmann, E. W. N. Glover, G. Heinrich, and H. Stenzel, Precise determination of the strong coupling constant at NNLO in QCD from the three-jet rate in electron-positron annihilation at LEP, *Phys. Rev. Lett.* **104**, 072002 (2010), arXiv:0910.4283 [hep-ph].
- [39] J. Schieck, S. Bethke, S. Kluth, C. Pahl, and Z. Trocsanyi (JADE), Measurement of the strong coupling α_{had} from the three-jet rate in e^+e^- annihilation using JADE data, *Eur. Phys. J. C* **73**, 2332 (2013), arXiv:1205.3714 [hep-ex].
- [40] G. Dissertori, A. Gehrmann-De Ridder, T. Gehrmann, E. W. N. Glover, G. Heinrich, G. Luisoni, and H. Stenzel, Determination of the strong coupling constant using matched NNLO+NLLA predictions for hadronic event shapes in e^+e^- annihilations, *JHEP* **08**, 036, arXiv:0906.3436 [hep-ph].
- [41] G. Abbiendi *et al.* (OPAL), Determination of α_s using OPAL hadronic event shapes at $\sqrt{s} = 91 - 209$ GeV and resummed NNLO calculations, *Eur. Phys. J. C* **71**, 1733 (2011), arXiv:1101.1470 [hep-ex].
- [42] S. Bethke, S. Kluth, C. Pahl, and J. Schieck (JADE), Determination of the Strong Coupling α_s from hadronic Event Shapes with $\mathcal{O}(\alpha_s^3)$ and resummed QCD predictions using JADE Data, *Eur. Phys. J. C* **64**, 351 (2009), arXiv:0810.1389 [hep-ex].
- [43] Z. Tulipánt, A. Kardos, and G. Somogyi, Energy-energy correlation in electron-positron annihilation at NNLL + NNLO accuracy, *Eur. Phys. J. C* **77**, 749 (2017), arXiv:1708.04093 [hep-ph].
- [44] K. Lee, A. Pathak, I. Stewart, and Z. Sun, Nonperturbative Effects in Energy Correlators: From Characterizing Confinement Transition to Improving α_s Extraction, (2024), arXiv:2405.19396 [hep-ph].
- [45] R. A. Davison and B. R. Webber, Non-Perturbative Contribution to the Thrust Distribution in e^+e^- Annihilation, *Eur. Phys. J. C* **59**, 13 (2009), arXiv:0809.3326 [hep-ph].
- [46] R. Abbate, M. Fickinger, A. H. Hoang, V. Mateu, and I. W. Stewart, Thrust at N^3LL with Power Corrections and a Precision Global Fit for $\alpha_s(m_Z)$, *Phys. Rev. D* **83**, 074021 (2011), arXiv:1006.3080 [hep-ph].
- [47] T. Gehrmann, G. Luisoni, and P. F. Monni, Power corrections in the dispersive model for a determination of the strong coupling constant from the thrust distribution, *Eur. Phys. J. C* **73**, 2265 (2013), arXiv:1210.6945 [hep-ph].
- [48] A. H. Hoang, D. W. Kolodrubetz, V. Mateu, and I. W. Stewart, Precise determination of α_s from the C -parameter distribution, *Phys. Rev. D* **91**, 094018 (2015), arXiv:1501.04111 [hep-ph].
- [49] G. Bell, C. Lee, Y. Makris, J. Talbert, and B. Yan, Effects of renormalon scheme and perturbative scale choices on determinations of the strong coupling from e^+e^- event shapes, *Phys. Rev. D* **109**, 094008 (2024), arXiv:2311.03990 [hep-ph].
- [50] H. Chen, P. F. Monni, Z. Xu, and H. X. Zhu, Scaling violation in power corrections to energy correlators from the light-ray OPE, (2024), arXiv:2406.06668 [hep-ph].
- [51] J. Andersen *et al.*, Les Houches 2023: Physics at TeV Colliders: Standard Model Working Group Report, in *Physics of the TeV Scale and Beyond the Standard Model: Intensifying the Quest for New Physics* (2024) arXiv:2406.00708 [hep-ph].
- [52] ATLAS Collaboration, Dependence of the jet energy scale on the particle content of hadronic jets in the atlas detector simulation, *JETM-2022-005* (2022).
- [53] ATLAS Collaboration, Dependence of the Jet Energy Scale on the Particle Content of Hadronic Jets in the ATLAS Detector Simulation, *ATL-PHYS-PUB-2022-021* (2022).
- [54] S. Gieseke, P. Stephens, and B. Webber, New formalism for QCD parton showers, *JHEP* **12**, 045, arXiv:hep-ph/0310083.
- [55] J. Bellm *et al.*, HERWIG 7.0/HERWIG ++ 3.0 release note, *Eur. Phys. J. C* **76**, 196 (2016), arXiv:1512.01178 [hep-ph].
- [56] S. Platzer and S. Gieseke, Coherent Parton Showers with Local Recoils, *JHEP* **01**, 024, arXiv:0909.5593 [hep-ph].
- [57] S. Platzer and S. Gieseke, Dipole Showers and Automated NLO Matching in Herwig++, *Eur. Phys. J. C* **72**, 2187 (2012), arXiv:1109.6256 [hep-ph].
- [58] S. Schumann and F. Krauss, A Parton shower algorithm based on Catani-Seymour dipole factorisation, *JHEP* **03**, 038, arXiv:0709.1027 [hep-ph].
- [59] T. Gleisberg, S. Hoeche, F. Krauss, M. Schonherr, S. Schumann, F. Siegert, and J. Winter, Event generation with SHERPA 1.1, *JHEP* **02**, 007, arXiv:0811.4622 [hep-ph].
- [60] E. Bothmann *et al.* (Sherpa), Event Generation with Sherpa 2.2, *SciPost Phys.* **7**, 034 (2019), arXiv:1905.09127 [hep-ph].
- [61] B. Andersson, G. Gustafson, G. Ingelman, and T. Sjostrand, Parton Fragmentation and String Dynamics, *Phys. Rept.* **97**, 31 (1983).
- [62] B. Andersson, *The Lund Model*, Cambridge Monographs on Particle Physics, Nuclear Physics and Cosmology, Vol. 7 (Cambridge University Press, 2023).
- [63] B. R. Webber, A QCD Model for Jet Fragmentation Including Soft Gluon Interference, *Nucl. Phys. B* **238**, 492 (1984).
- [64] P. Skands, S. Carrazza, and J. Rojo, Tuning PYTHIA 8.1: the Monash 2013 Tune, *Eur. Phys. J. C* **74**, 3024 (2014), arXiv:1404.5630 [hep-ph].
- [65] J.-C. Winter, F. Krauss, and G. Soff, A Modified cluster hadronization model, *Eur. Phys. J. C* **36**, 381 (2004), arXiv:hep-ph/0311085.
- [66] G. S. Chahal and F. Krauss, Cluster Hadronisation in Sherpa, *SciPost Phys.* **13**, 019 (2022), arXiv:2203.11385 [hep-ph].

- [67] J. de Favereau, C. Delaere, P. Demin, A. Giammanco, V. Lemaitre, A. Mertens, and M. Selvaggi, Delphes 3: a modular framework for fast simulation of a generic collider experiment, *Journal of High Energy Physics* **2014**, 10.1007/jhep02(2014)057 (2014).
- [68] C. Chen, X. Mo, M. Selvaggi, Q. Li, G. Li, M. Ruan, and X. Lou, Fast simulation of the CEPC detector with Delphes, (2017), arXiv:1712.09517 [hep-ex].
- [69] A. Abada *et al.* (FCC), FCC-ee: The Lepton Collider: Future Circular Collider Conceptual Design Report Volume 2, *Eur. Phys. J. ST* **228**, 261 (2019).
- [70] J. Jiang, S. Zhao, Y. Niu, Y. Shi, Y. Liu, D. Han, T. Hu, and B. Yu, Study of SiPM for CEPC-AHCAL, *Nucl. Instrum. Meth. A* **980**, 164481 (2020).
- [71] M. Aleksa, F. Bedeschi, R. Ferrari, F. Sefkow, and C. G. Tully, Calorimetry at FCC-ee, *Eur. Phys. J. Plus* **136**, 1066 (2021), arXiv:2109.00391 [hep-ex].
- [72] M. Dong *et al.* (CEPC Study Group), CEPC Conceptual Design Report: Volume 2 - Physics & Detector, (2018), arXiv:1811.10545 [hep-ex].
- [73] C. A. S. Group, Snowmass2021 white paper af3-cepc (2022), arXiv:2203.09451 [physics.acc-ph].
- [74] Y. Zhu, S. Chen, H. Cui, and M. Ruan, Requirement analysis for dE/dx measurement and PID performance at the CEPC baseline detector, *Nucl. Instrum. Meth. A* **1047**, 167835 (2023), arXiv:2209.14486 [physics.ins-det].